Effect of pressure on electron transfer reactions in inorganic and bioinorganic chemistry

ARTICLE *in* BIOCHIMICA ET BIOPHYSICA ACTA · APRIL 2002

Impact Factor: 4.66 · DOI: 10.1016/S0167-4838(01)00351-X · Source: PubMed

2 AUTHORS:

Joanna Macyk
Friedrich-Alexander-University of Erlangen-…
5 PUBLICATIONS **43** CITATIONS
SEE PROFILE

Rudi van Eldik
Friedrich-Alexander-University of Erlangen-…
885 PUBLICATIONS **16,833** CITATIONS
SEE PROFILE

ELSEVIER

Biochimica et Biophysica Acta 1595 (2002) 283–296

BIOCHIMICA ET BIOPHYSICA ACTA
BBA

www.bba-direct.com

Review

Effect of pressure on electron transfer reactions in inorganic and bioinorganic chemistry

Joanna Macyk, Rudi van Eldik *

Institute for Inorganic Chemistry, University of Erlangen-Nürnberg, Egerlandstrasse 1, 91058 Erlangen, Germany

Received 3 September 2001; received in revised form 20 November 2001; accepted 21 November 2001

Abstract

Kinetic and thermodynamic studies involving the application of different high-pressure techniques, are very useful in gaining mechanistic information on the basis of volume changes that occur during inorganic and bioinorganic electron transfer reactions. The most fundamental type of electron transfer reaction concerns self-exchange reactions, for which the overall reaction volume is zero, and activation volumes can be measured and discussed. In the case of non-symmetrical electron transfer reactions, intra- and intermolecular processes can be studied and volume profiles can be constructed. Precursor complex formation can in some cases be recognized kinetically in such systems. Typical values of activation and reaction volumes are reviewed for various reversible and irreversible electron transfer reactions. Mechanistic conclusions reached on the basis of these parameters are presented. Volume profiles for electron transfer reactions enable a simplistic presentation of the reaction mechanism on the basis of intrinsic and solvational volume changes along the reaction coordinate.

Keywords: Pressure effect; Electron transfer reaction; Activation volume; Reaction volume; Volume profile

1. Introduction

The value of mechanistic information that emerges from kinetics measurements over a series of elevated pressures for solution reactions in inorganic chemistry has been realized for some time [1]. However, many inorganic reactions are too fast to follow using conventional instrumentation. Hence the momentum regarding investigations at high pressures vis-a-vis organic reactions was delayed somewhat until adaptation of rapid reaction techniques for operation at high pressures had been achieved, mostly in the period from 1975 to 1985. This fertile period has been recorded in reviews, in conference proceedings, and in monographs, and readers may obtain a thorough background and sense of historical development by consulting this literature [2–13]. Even until quite recently, suitable instrumentation was not widely available.

The purpose of this article is to familiarize the reader with the current status of activities in the application of hydrostatic pressure to mechanistic studies on electron transfer reactions in inorganic chemistry, as well as in the blossoming field of bioinorganic chemistry. Since this is not intended to be a comprehensive review, only a selection of representative reactions and typical examples, in

* Corresponding author.

0167-4838/02/$ – see front matter
PII: S0167-4838(01)00351-X

many cases from our own work in this area, will be described. The basic principles involved in high-pressure kinetics for reactions in general have been the subject of many reports [14–16].

The parameter that is derived from high-pressure kinetic experiments in solution when the transition state theory applies, is the difference in partial molar volume between the activated complex of transition state theory and the reactant state, and is known as the volume of activation, $\Delta V^{\#}$. If the particular reaction is reversible and the system experimentally accessible, $\Delta V^{\#}$ for the reverse reaction can also be obtained and thus, except for solvent exchange and self-exchange electron transfer reactions in which there is no net volume change, the difference between these two quantities results in the reaction volume, ΔV. The latter quantity, in some cases, may also be determined by measuring the equilibrium constant (K) for the reaction as a function of pressure or from the partial molar volumes of the reactants and products, derived from solution density measurements. The volume of activation itself is determined from measurements of the reaction rate constant k at different hydrostatic pressures p at a given absolute temperature T, since $(\partial \ln k/\partial p)_T = -\Delta V^{\#}/RT$ (R is the ideal gas constant), an equation developed within transition state theory based upon the analogous equilibrium constant relationship $(\partial \ln K/\partial p)_T = -\Delta V/RT$. The former equation, upon integration, can be employed to determine $\Delta V^{\#}$ from a plot of $\ln k$ versus p. Providing the pressure is no higher than 200 MPa, in the vast majority of cases $\Delta V^{\#}$ is pressure independent and the plot is linear. A non-linear behavior is usually encountered when dealing with a compressible solvent where both the reaction and activation volume become pressure sensitive. In this article the focus will be on reactions in which there is a negligible or absence of pressure dependence of the volume of activation. In general, volume of activation data quoted in this report will refer to ambient conditions, i.e., close to room temperature, and readers are advised to consult the cited literature for more detailed information on the exact experimental conditions employed.

Equilibrium and kinetic parameters obtained as a function of temperature permit the drawing of diagrams illustrating the Gibbs free energy (G), enthalpy (H) and entropy (S) changes in proceeding in the sequence reactant state/transition state/product state, and including intermediates when they are formed. Correspondingly, a volume diagram or volume profile can chart the respective volume changes along the reaction coordinate, and when appropriate actual partial molar volumes are known, on an absolute rather than a relative basis, something realizable for S, but not for H and G. Hence if reactants A and B form a product AB and no intermediates are formed, i.e., there is a single-step reaction, a volume profile in which the reaction volume is, for example, negative and the volume of activation is such that the transition state is almost halfway between reactant and product states, is depicted in Fig. 1.

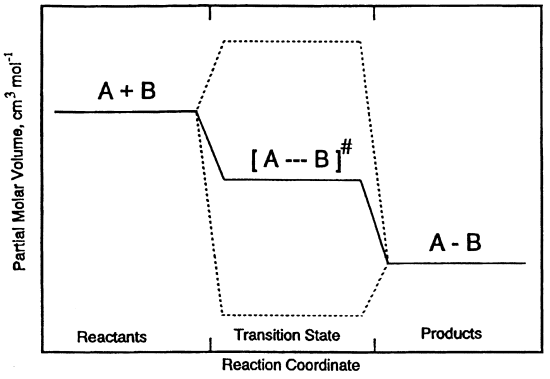

Fig. 1. Volume profile for the overall reaction A+B→AB. The activated complex is [A- - -B]$^{\#}$.

As shown in Fig. 1, other forms of the volume profile are possible depending on the particular character of the system. Thus, in principle, a volume profile represents a simple and lucid way of describing a reaction and diagnosing the mechanism, but with the caveat that mechanistic diagnosis is uncomplicated when only intrinsic changes (changes in bond lengths, bond angles for example) occur. In many actual reactions, when charged species are produced or neutralized during the reaction, or increases or decreases in polarity occur, then there is also a change in the volume occupied by the solvent molecules surrounding the system by virtue of an increase or decrease in (at least) the first solvation layer. Volume reduction of solvent from this source is known as electrostriction. Thus the facile interpretation of measured values of ΔV or $\Delta V^{\#}$ can be compromised by the existence of the two and difficulty quantifiable contributions.

2. Electron-transfer reactions

A fundamental understanding of oxidation–reduction reactions is vital to the inorganic chemist in the context of energy transduction, corrosion processes, metallurgy, redox processes in environmental chemistry, and metalloenzymes and metalloproteins involved in electron transfer. Electron-transfer reactions of transition metal complexes are accompanied by a change in the oxidation state of the metal atom and the overall charge on the complex ion. This can cause both intrinsic and solvational volume changes, such that it is reasonable to expect that electron-transfer reactions should exhibit characteristic volumes of activation.

In the following sections the effect of pressure on different types of electron-transfer processes will be discussed systematically. Some of our work in this area was reviewed as part of a special symposium devoted to the complementarity of various experimental techniques in the study of electron transfer reactions [17]. Swaddle and Tregloan recently reviewed electrode reactions of metal complexes in solution at high pressure [12]. The main emphasis in this section will fall on some of the most recent work that we have been involved in, dealing with 'long-distance' electron-transfer processes involving cytochrome *c*. However, by way of introduction, a short discussion on the effect of pressure on self-exchange (symmetrical) and non-symmetrical electron-transfer reactions between transition metal complexes that have been reported in the literature, will be presented.

3. Self-exchange reactions

Self-exchange reactions are the most simple type of electron-transfer reactions, they are symmetrical processes for which both the reaction free energy and reaction volume are zero, and ideal for theoretical modeling. They form the basis for much of the discussion and interpretation of non-symmetrical reactions in a similar way as solvent exchange reactions form a basis for the understanding of ligand substitution reactions. Swaddle and co-workers have made a significant contribution in this area. They have studied the effect of pressure on the self-exchange

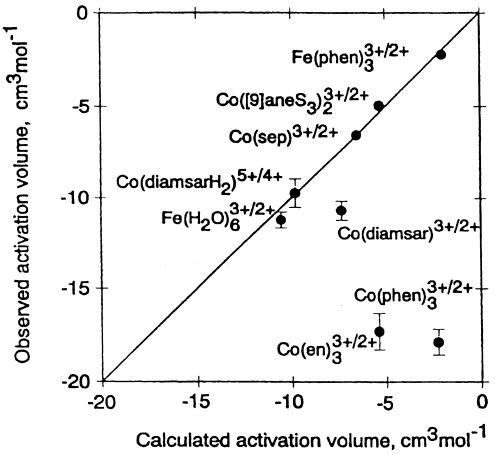

Fig. 2. Plot of $\Delta V^{\#}$(observed) versus $\Delta V^{\#}$(calculated) for a series of self-exchange electron-transfer reactions.

reactions (volumes of activation are quoted in brackets in $cm^3\ mol^{-1}$) $[Fe(H_2O)_6]^{3+/2+}$ (−11.1) [18], $[Fe(phen)_3]^{3+/2+}$ (−2.2) [18], $[Fe(CN)_6]^{3-/4-}$ (+22) [19], $[MnO_4]^{2-/-}$ (−23) [20], $[Co(sep)]^{3+/2+}$ (−6.4) [21], $[Co([9]aneS_3)]^{3+/2+}$ (−4.8) [21], $[Co(diamsarH_2)]^{5+/4+}$ (−9.6) [22], $[Co(diamsar)]^{3+/2+}$ (−10.4) [22], $[Co(en)_3]^{3+/2+}$ (−15.5) [23], and $[Co(phen)_3]^{3+/2+}$ (−17.6) [24]. In the majority of cases the self-exchange reaction is significantly accelerated by pressure, with the exception of the $[Fe(CN)_6]^{3-/4-}$ system which goes in exactly the opposite way, and the observed volume of activation is in agreement with the significantly negative entropy of activation reported for such systems. In addition, they have also gone through impressive efforts to calculate the volumes of activation theoretically based on the Marcus–Hush–Stranks treatment and their own modifications and additions [25,26]. For a large number of systems a good agreement between the experimental and theoretically calculated volumes of activation were found as shown in Fig. 2.

In most cases solvent reorganization accounts for the largest contribution towards the observed volume of activation. Large deviations were found only for the $[Co(en)_3]^{3+/2+}$ and $[Co(phen)_3]^{3+/2+}$ systems where the theoretical volume of activation is between 10 and 15 $cm^3\ mol^{-1}$ more positive than the experimental value [23,24]. This deviation is most probably related to the participation of a high-spin to low-spin changeover associated with the electron-

transfer process, which can account for an additional volume collapse of ca. 10 to 15 cm^3 mol^{-1} [22].

$$MnO_4^- + MnO_4^{2-} \rightarrow MnO_4^{2-} + MnO_4^- \quad (1)$$

A notable feature of anion-anion electron transfer reactions such as that of Reaction 1 and also in non-symmetrical reactions described below, is the fact that some alkali metal ions can catalyze the electron transfer process [27–31]. Thus far in most cases no detailed explanation from the point of view of volume changes is available since extraction of the volumes of activation for the catalyzed and uncatalyzed pathways from the high-pressure kinetics results is often not possible. Lithium ions yield no catalytic influence, and the effect is only modest or very small when sodium ions are present in the case of Reaction 1. However, lithium ions do have a significant catalytic effect, and sodium ions quite a substantial one, on cyanometalate self-exchange reactions in water [30]. Reaction acceleration is quite pronounced in the presence of potassium ions, even more so when Rb^+ or NH_4^+ are present in examples where they have been employed. The catalysis no doubt arises from the cation shielding the repulsion between the anionic partners. However, it is not yet established which specific property such as the radius or the charge density results in efficient catalysis by some ions and not by others. In the case of Reaction 1, where the observed $\Delta V^{\#}$ for the uncatalyzed path equals -21 cm^3 mol^{-1} and the observed rate constant has been dissected into the values for the catalyzed and uncatalyzed pathways, it is clear that the catalyzed path involves a dramatically lower volume change in reaching the transition state ($\Delta V^{\#} = +3$ cm^3 mol^{-1} (Na^+) and -1 cm^3 mol^{-1} (K^+)) [20]. The catalytic efficiency may be correlated with the polarizability of M^+ or with the inverse of the hydrated ion ($M(aq)^+$) radius. In the uncatalyzed path the volume reduction may be regarded as arising from the compression of the ellipsoidal solvent cavity in which the two ions are enclosed and the closer approach of the two Mn centers. The solvational effects are much less in the cation catalyzed pathway.

More recently, Swaddle and coworkers [32–34] have demonstrated that for aqueous systems a good correlation exists between the volume of activation for a homogeneous self-exchange reaction and the activation volume for the heterogeneous self-exchange reaction at an electrode. The slope of the line in Fig. 3 for 10 sets of data is 0.50 and in precise agreement with an extension of the Marcus theory. This led the authors to suggest a 'fifty percent rule' with which volume of activation data can be predicted for self-exchange reactions, which cannot be measured directly for technical reasons, on the basis of electrochemical data recorded as a function of pressure.

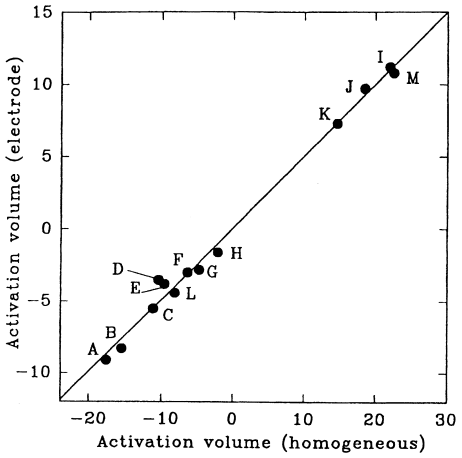

Fig. 3. Plot of $\Delta V^{\#}$(electrode) versus $\Delta V^{\#}$(homogeneous) for a series of self-exchange couplets: A, $Co(phen)_3^{3+/2+}$; B, $Co(en)_3^{3+/2+}$; C, $Fe(H_2O)_6^{3+/2+}$; D, $Co(diamsar)^{3+/2+}$; E, $Co(diamsarH_2)^{5+/4+}$; F, $Co(sep)^{3+/2+}$; G, $Co(ttcn)_2^{3+/2+}$; H, $Fe(phen)_3^{3+/2+}$; I, $Fe(CN)_6^{3-/4-}$; J, $Os(CN)_6^{3-/4-}$; K, $Mo(CN)_8^{3-/4-}$; L, $Mo(CN)_8^{3-/4-}$; M, $W(CN)_8^{3-/4-}$.

The above quoted reactions all proceed via an outer-sphere electron-transfer mechanism. By way of comparison, the volume of activation for the exchange reaction in $[Fe(H_2O)_5OH]^{2+}/[Fe(H_2O)_6]^{2+}$ was reported to be +0.8 cm^3 mol^{-1}, i.e., significantly more positive than found for $[Fe(H_2O)_6]^{3+/2+}$ [18]. This difference was ascribed to the release of a solvent molecule associated with the formation of an hydroxo-bridged intermediate in terms of an inner-sphere mechanism.

4. Non-symmetrical reactions

For the mechanistic interpretation of activation volume data for non-symmetrical electron-transfer reactions, it is essential to have information on the overall volume change that can occur during such a process. This then enables the construction of a vol-

ume profile for the electron transfer process and allows a detailed interpretation of the activation volume in terms of the overall volume associated with the reaction. The reaction volume can be calculated from the partial molar volumes of reactant and product species, when these are available, or can be determined from density measurements. Efforts have in recent years focused on the electrochemical determination of reaction volume data from the pressure dependence of the redox potential. Tregloan and coworkers [35,36] have demonstrated how such techniques can reveal information on the magnitude of intrinsic and solvational volume changes associated with electron-transfer reactions of transition metal complexes. The measured reaction volumes have to be corrected for the effect of pressure on the reference electrode, for which they conducted a well-designed set of experiments on a series of $Fe^{II/III}$ couples in which the ligands were systematically varied in order to adjust the overall charge of the complex, and therefore the solvational contribution towards the overall reaction volume. A good correlation was found between the reaction volume and the difference in the square of the charge on the oxidized and reduced forms of the complex as shown in Fig. 4 [35]. By interpolation to $\Delta z^2 = 0$, the reaction volume for the Ag/Ag^+ reference electrode was determined to be -11.9 ± 0.5 cm^3 mol^{-1}. Measurements on a series of Cr, Co and Ru complexes enabled a systematic differentiation to be made between intrinsic and solvational volume contributions associated with the redox process [36].

It has in general been the objective of many mechanistic studies dealing with inorganic electron-transfer reactions to distinguish between outer-sphere (intermolecular) and inner-sphere (intramolecular) mechanisms, since these describe the way the reactants interact with each other prior to electron transfer. In the case of electron-transfer reactions between proteins, the location of the protein at a specific site usually leads to an intramolecular electron-transfer process. Along these lines high-pressure kinetic methods and the construction of reaction volume profiles have also been employed to contribute towards a better understanding of the intimate mechanisms involved in such processes. The differentiation between outer-sphere and inner-sphere mechanisms depends on the nature of the precursor species, Ox//Red in

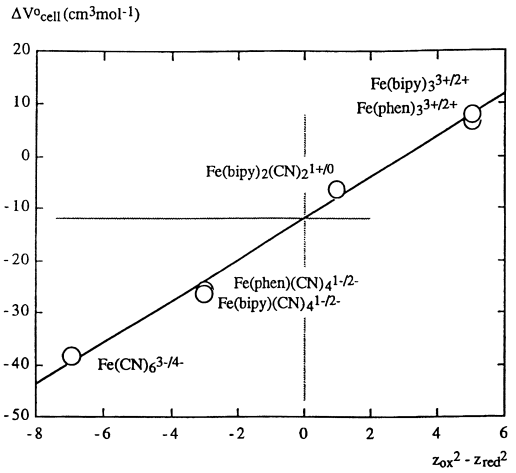

Fig. 4. Plot of $\Delta V°_{cell}$ versus $Z^2_{ox} - Z^2_{red}$ for a series of Fe(II)/Fe(III) redox systems.

the following scheme, which can either be an ion pair or encounter complex, or a bridged intermediate, respectively.

$$Ox + Red \rightleftharpoons Ox//Red,\ K \tag{2}$$

$$Ox//Red \rightarrow Ox^-//Red^+,\ k_{ET} \tag{3}$$

$$Ox^-//Red^+ \rightleftharpoons Ox^- + Red^+ \tag{4}$$

The coordination sphere of the reactants remains intact in the former case and is modified by ligand substitution in the latter, which will naturally affect the associated volume changes.

A general difficulty encountered in kinetic studies of outer-sphere electron-transfer processes concerns the separation of the precursor formation constant (K) and the electron-transfer rate constant (k_{ET}) in the reactions outlined above. In the majority of cases, precursor formation is a diffusion controlled step, followed by rate-determining electron transfer. In the presence of an excess of Red, the rate expression is given by:

$$k_{obs} = k_{ET}K[Red]/(1 + K[Red]) \tag{5}$$

In many cases K is small, such that this equation simplifies to $k_{obs} = k_{ET}K[Red]$, which means that the observed second-order rate constant and the associated activation parameters are composite quantities, viz. $\Delta V^{\#} = \Delta V^{\#}(k_{ET}) + \Delta V(K)$. When K is large enough such that $1 + K[Red] > 1$, it is possible to separate k_{ET} and K kinetically and also the associated activation

parameters, viz. $\Delta V^{\#}(k_{ET})$ and $\Delta V(K)$ [37]. A series of reactions were studied where it was possible to resolve K and k_{ET}, i.e., $\Delta V(K)$ and $\Delta V^{\#}(k_{ET})$. In this case oppositely charged reaction partners were selected as indicated in the following reactions [38–40]:

$$[Co(NH_3)_5X]^{(3-n)+} + [Fe(CN)_6]^{4-} \rightleftharpoons \{Co(NH_3)_5X^{(3-n)+}, Fe(CN)_6^{4-}\},\ K \quad (6)$$

$$\{Co(NH_3)_5X^{(3-n)+}, Fe(CN)_6^{4-}\} \rightarrow Co^{2+} + 5NH_3 + X^{n-} + [Fe(CN)_6]^{3-},\ k_{ET} \quad (7)$$

$$X^{n-} = H_2O,\ Me_2SO,\ py,\ Cl^-, N_3^-$$

Throughout the series, ion-pair formation is accompanied by significantly negative $\Delta S°$ values and close to zero ΔV values. The latter is rather surprising, since it is generally accepted that ion-pair formation should involve considerable charge neutralization accompanied by strong desolvation due to a decrease in electrostriction. The values of ΔV therefore indicate that the reaction partners most probably exist as solvent-separated ion pairs, i.e., with no significant charge neutralization accompanied by desolvation. The activation parameters demonstrate that the electron-transfer steps exhibit a strong pressure deceleration, most systems have a $\Delta V^{\#}$ value of between +25 and +34 $cm^3\ mol^{-1}$. These values indicate that electron transfer is accompanied by extensive desolvation, most probably related to charge neutralization associated with the electron-transfer process [40]. A simplified model based on partial molar volume data, in which electron transfer occurs from the precursor ion pair $\{Co(NH_3)_5X^{(3-n)+},Fe(CN)_6^{4-}\}$ to the successor ion pair $\{Co(NH_3)_5X^{(2-n)+},Fe(CN)_6^{3-}\}$, predicts an overall volume increase of ca. 65 $cm^3\ mol^{-1}$. This means that according to the reported $\Delta V^{\#}$ values the transition state for the electron-transfer process lies approximately halfway between the reactant and product states on a volume basis for the precursor and successor ion pairs. The largest volume contribution arises from the oxidation of $[Fe(CN)_6]^{4-}$ to $[Fe(CN)_6]^{3-}$, which is accompanied by a large decrease in electrostriction and an increase in partial molar volume. Theoretical calculations also confirmed that the transition state for these reactions lies approximately halfway along the reaction coordinate on a volume basis [40]. This first information on the nature of the volume profile for an outer-sphere electron-transfer reaction proved to be in good agreement with subsequently reported results for systems with low driving forces in which it was possible to construct a complete volume profile by studying the effect of pressure on both the forward and reverse reactions, as well as on the overall equilibrium constant (see further discussion). Data have also been reported for a series of related complexes containing phosphor-oxo ligands [41–43], and the results can be interpreted in terms of major solvational changes associated with the oxidation of $[Fe(CN)_6]^{4-}$.

5. Bioinorganic reactions

A number of electron transfer reactions of biological interest have been studied using high-pressure techniques [2,3]. These include the oxidation of L-ascorbic acid by $[Fe(CN)_6]^{3-}$ [44], $[Fe(CN)_5NO_2]^{3-}$ [45], and $Fe(phen)_2(CN)_2]^-$ [46]. The first two reactions are characterized by volumes of activation of -16 and $-10\ cm^3\ mol^{-1}$, respectively, which indicate that solvent rearrangement as a result of an increase in electrostriction must account for the volume collapse on going to the transition state. In comparison, the third reaction exhibited almost no pressure dependence, in line with significantly less charge formation than in the case of the 3-charged complexes. The oxidation of deoxy- and oxymyoglobin by $[Fe(CN)_6]^{3-}$ was also studied as a function of pressure [47]. The oxidation of deoxymyoglobin is ca. seven times faster than the oxidation of oxymyoglobin at 298 K, and the corresponding volume of activation, determined under limiting kinetic conditions, is $-20\ cm^3\ mol^{-1}$. This value is in good agreement with that reported above for the reduction of $[Fe(CN)_6]^{3-}$ to $[Fe(CN)_6]^{4-}$. The oxidation of oxymyoglobin is characterized by an activation volume of $-3\ cm^3\ mol^{-1}$, which must be corrected for the reaction volume of $-19\ cm^3\ mol^{-1}$ associated with the binding of dioxygen to myoglobin [48]. The resulting $-22\ cm^3\ mol^{-1}$ is once again in good agreement with that expected for the reduction of $[Fe(CN)_6]^{3-}$.

A challenging question concerns the feasibility of

the application of high-pressure kinetic and thermodynamic techniques in the study of such reactions. Do 'long-distance' electron transfer processes exhibit a characteristic pressure dependence, and to what extent can a volume profile analysis reveal information on the intimate mechanism?

The systems that we investigated in collaboration with others involved intermolecular and intramolecular electron-transfer reactions between ruthenium complexes and cytochrome *c*. We also studied a series of intermolecular reactions between chelated cobalt complexes and cytochrome *c*. A variety of high-pressure experimental techniques, including stopped-flow, flash-photolysis, pulse-radiolysis and voltammetry, were employed in these investigations. As the following presentation will show, a remarkably good agreement was found between the volume data obtained with the aid of these different techniques, which clearly demonstrates the complementarity of these methods for the study of electron-transfer processes.

Application of pulse-radiolysis techniques revealed that the following intramolecular and intermolecular electron-transfer reactions all exhibit a significant acceleration with increasing pressure. The reported volumes of activation are -17.7 ± 0.9, -18.3 ± 0.7, and -15.6 ± 0.6 cm^3 mol^{-1}, respectively, and clearly demonstrate a significant volume collapse on going from the reactant to the transition state [49].

$$(NH_3)_5Ru^{II}-(His33)cyt\ c^{III} \rightarrow (NH_3)_5Ru^{III}-(His33)cyt\ c^{II} \quad (8)$$

$$(NH_3)_5Ru^{II}-(His39)cyt\ c^{III} \rightarrow (NH_3)_5Ru^{III}-(His39)cyt\ c^{II} \quad (9)$$

$$[Ru^{II}(NH_3)_6]^{2+} + cyt\ c^{III} \rightarrow [Ru^{III}(NH_3)_6]^{3+} + cyt\ c^{II} \quad (10)$$

At this stage it was uncertain what the negative volumes of activation really meant since overall reaction volumes were not available. There were, however, data, now in the literature [36], that suggested that the oxidation of $[Ru(NH_3)_6]^{2+}$ to $[Ru(NH_3)_6]^{3+}$ is accompanied by a volume decrease of ca. 30 cm^3 mol^{-1}, which would mean that the activation volumes quoted above could mainly arise from volume changes associated with the oxidation of the ruthenium redox partner.

In order to obtain further information on the magnitude of the overall reaction volume and the location of the transition state along the reaction coordinate, a series of intermolecular electron-transfer reactions of cytochrome *c* with pentaammineruthenium complexes were studied, where the sixth ligand on the ruthenium complex was selected in such a way that the overall driving force was low enough so that the reaction kinetics could be studied in both directions [50,51]. The selected substituents were isonicotinamide (isn), 4-ethylpyridine (etpy), pyridine (py), and 3,5-lutidine (lut). The overall reaction can be formulated as:

$$[Ru^{III}(NH_3)_5L]^{3+} + cyt\ c^{II} \rightleftharpoons [Ru^{II}(NH_3)_5L]^{2+} + cyt\ c^{III} \quad (11)$$

For all the investigated systems, the forward reaction was significantly decelerated by pressure, whereas the reverse reaction was significantly accelerated by pressure. The absolute values of the volumes of activation for the forward and reverse processes were indeed very similar, demonstrating that a similar rearrangement occurs in order to reach the transition state. In addition, the overall reaction volume for these systems could be determined spectrophotometrically by recording the spectrum of an equilibrium mixture as a function of pressure, and electrochemically by recording cyclic and differential pulse voltammograms as a function of pressure [52]. A comparison of the ΔV data demonstrates the generally good agreement between the values obtained from the difference in the volumes of activation for the forward and reverse reactions, and those obtained thermodynamically. Furthermore, the values also clearly demonstrate that $|\Delta V^{\#}| \approx 0.5|\Delta V|$, i.e., the transition state lies approximately halfway between the reactant and product states on a volume basis independent of the direction of electron transfer. The typical volume profile in Fig. 5 presents the overall picture, from which the location of the transition state can clearly be seen.

Similar results were obtained for the redox reactions of a series of cobalt diimine complexes with cytochrome *c* [53,54]. In general, a good agreement exists between the kinetically and thermodynamically

determined parameters, and the typical volume profile in Fig. 6 once again demonstrates the symmetrical location of the transition state with respect to the reactant and product states.

At this point it is important to ask the question where these volume changes really come from. We have always argued that the major volume change arises from changes on the redox partner and not on cytochrome *c* itself. This was suggested by the fact that the change in partial molar volume associated with the oxidation of the investigated Ru(II) and Co(II) complexes as obtained from electrochemical and density measurements, almost fully accounted for the observed overall reaction volume. Thus the reduction of cytochrome *c* can only make a minor contribution towards the overall volume change.

These arguments were apparently in contradiction with electrochemical results reported by Cruanes et al. [55], according to which the reduction of cytochrome *c* is accompanied by a volume collapse of 24 cm^3 mol^{-1}. This value is so large that it almost represents all of the reaction volume found for the investigated reactions discussed above. A reinvestigation of the electrochemistry of cytochrome *c* as a function of pressure, using cyclic and differential pulse voltammetric techniques [52], revealed a reaction volume of -14.0 ± 0.5 cm^3 mol^{-1} for the reaction

$$\text{cyt } c^{III} + Ag(s) + Cl^- \rightarrow \text{cyt } c^{II} + AgCl(s) \qquad (12)$$

A correction for the contribution from the reference electrode can be made on the basis of the data published by Tregloan et al. [35], and a series of measurements of the potential of the Ag/AgCl(KCl sat'd) electrode relative to the Ag/Ag^+ electrode as a function of pressure. The contribution of the reference electrode turned out to be -9.0 ± 0.6 cm^3 mol^{-1}, from which it then followed that the reduction of cytochrome c^{III} is accompanied by a volume decrease of 5.0 ± 0.8 cm^3 mol^{-1}. This contribution is significantly smaller than concluded by Cruanes et al. [55], and is also in line with the other arguments referred to above. Thus we conclude that the observed activation and reaction volumes mainly arise from volume changes on the Ru and Co complexes, which in turn will largely be associated with changes in electrostriction in the case of the ammine complexes. The oxidation of the Ru(II) ammine complexes will be accompanied by a large increase in electrostriction and almost no change in the metal–ligand bond length, whereas in the case of the Co complexes a significant contribution from intrinsic volume changes associated with the oxidation of Co(II) will partially account for the observed effects [36].

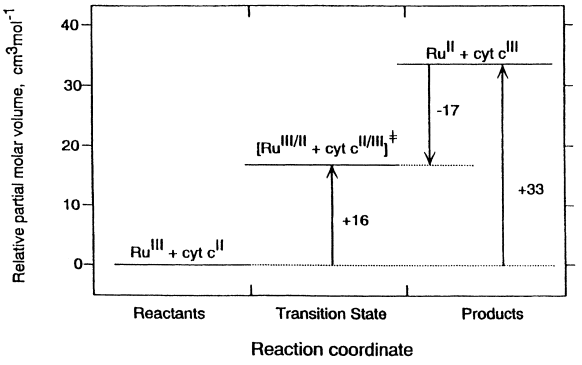

Fig. 5. Volume profile for the reaction $Ru(NH_3)_5isn^{3+}$+cyt $c^{II} \rightleftharpoons Ru(NH_3)_5isn^{2+}$+cyt c^{III}.

The available results nicely demonstrate the complementarity of the kinetic and thermodynamic data obtained from stopped-flow, UV-vis, electrochemical and density measurements. The resulting picture is very consistent and allows a further detailed analysis of the data. The overall reaction volumes determined in four different ways are surprisingly similar and underline the validity of the different methods employed. The volume profiles in Figs. 5 and 6 demonstrate the symmetric nature of the intrinsic and solvational reorganization in order to reach the

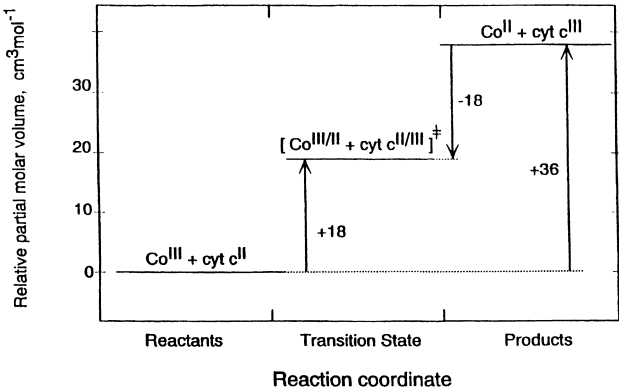

Fig. 6. Volume profile for the reaction $Co(terpy)_2^{3+}$+cyt $c^{II} \rightleftharpoons Co(terpy)_2^{2+}$+cyt c^{III}.

transition state of the electron-transfer process. In these systems the volume profile is controlled by effects on the redox partner of cytochrome *c*, but this does not necessarily always have to be the case. The location of the transition state on a volume basis will reveal information concerning the 'early' or 'late' nature of the transition state and reveal details of the actual electron-transfer route followed.

In the above quoted examples involving cytochrome *c*, precursor formation between the reactants is too weak to enable the kinetic separation of the precursor formation constant K and the electron transfer rate constant k_{ET}, with the result that the observed second-order rate constant is a composite quantity and represents $k_{ET}K$. For this reason much attention was paid in subsequent studies to reactions in which the separation of these constants should in principle be possible. Under conditions of effective precursor formation (for instance in the case of reaction partners of opposite charge), saturation kinetics should be observed for which the electron transfer reaction then represents the limiting rate constant.

The first example is the irreversible reaction between the anionic *trans*-bis(2-ethyl-2-hydroxybutanoato(2-))oxochromate(V) complex and cytochrome c^{II} as given in Reaction 13 [56].

$$[Cr^{V}(L)_2]^{1-} + \text{cyt } c^{II} \rightarrow [Cr^{IV}(L)_2]^{2-} + \text{cyt } c^{III} \quad (13)$$

$$L = 2-\text{ethyl}-2-\text{hydroxybutanoato}(2-)$$

The low stability of the chromium complex complicated the experimental measurements at high complex concentrations. Nevertheless, the concentration dependence of the observed pseudo-first order rate constant showed clear saturation kinetics, for which $K = 37 \pm 5$ M^{-1} and $k_{ET} = 1510 \pm 170$ s^{-1} at pH 4.8 and 15°C. The thermal activation parameters determined in the low concentration range (i.e., where the second-order rate constant equals Kk_{ET}), show a low value for the activation enthalpy, $\Delta H^{\neq} = 20.9 \pm 0.6$ kJ mol^{-1}, and a high negative value for the activation entropy, $\Delta S^{\neq} = -80 \pm 2$ J K^{-1} mol^{-1}. The significantly negative activation entropy suggests a highly-structured transition state. What can we say about the location of the transition state in terms of volume changes along the reaction coordinate?

The activation volumes were found to be -9.2 ± 0.6 and -11.1 ± 0.8 cm^3 mol^{-1} at pH 5.0 and 4.8, respectively. From electrochemical measurements on the $Cr^{V/IV}$ couple, the dependence of the redox potential on pressure was determined, from which reaction volumes of -11.8 ± 0.5 (pH 5.0) and -14.7 ± 0.7 cm^3 mol^{-1} (pH 4.8) for this redox couple could be calculated. In this case the overall volume changes result from the reduction of Cr^{V} to Cr^{IV}, and the change in the overall charge from -1 to -2. From earlier electrochemical studies it is known that the oxidation of cytochrome c^{II} to cytochrome c^{III} is accompanied by a small volume increase of 5.0 ± 0.8 cm^3 mol^{-1} [52]. It follows that the overall oxidation of cytochrome c^{II} by the Cr^{V} oxo species is associated with an overall volume decrease of 7 and 10 cm^3 mol^{-1}, respectively. The solvational effects arising from the increase in electrostriction account for the overall negative reaction volumes. The volume profile for electron transfer in this system exhibits a non-symmetrical nature as shown in Fig. 7. The transition state lies on the product side and can be characterized as 'late' [56].

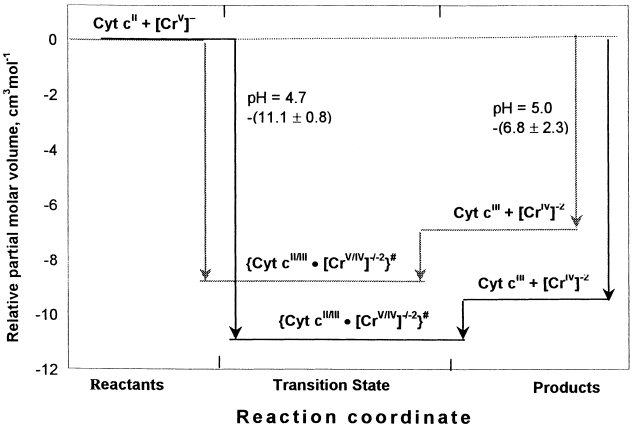

Fig. 7. Volume profile for the reaction of cyt c^{II} with *trans*-bis(2-ethyl-2-hydroxybutanoato(2-))oxochromate(V).

Saturation kinetics were also found for the irreversible reaction between cytochrome c^{II} and trisoxalatocobalt(III) as shown in Reaction 14 [57].

$$[Co^{III}(ox)_3]^{3-} + \text{cyt } c^{II} \rightarrow [Co^{II}(ox)_3]^{4-} + \text{cyt } c^{III} \quad (14)$$

The activation volume for the combined formation of the ion-pair and subsequent electron transfer reaction was obtain for low concentrations of the co-

balt complex and found to be $\Delta V^{\neq} = \Delta V(K) + \Delta V^{\neq}(k_{ET}) = -11 \pm 1$ cm^3 mol^{-1}, since $k_{obs} = Kk_{ET}$-[Co^{III}] under these conditions. At high Co(III) concentrations, $\Delta V^{\neq}(k_{ET})$ was found to be -5.5 ± 0.6 cm^3 mol^{-1}, since $k_{obs} = k_{ET}$ under such conditions. The $\Delta H^{\neq}$ and $\Delta S^{\neq}$ values are larger and $\Delta V^{\neq}$ is more negative for lower concentrations of $[Co(ox)_3]^{3-}$, i.e., under conditions where the two steps of the reaction contribute to these values. At the high concentration limit only the electron transfer process determines the activation parameters.

The difference between the $\Delta V^{\neq}$ data reported for the reaction at high and low trisoxalatocobalt(III) concentrations, represents the value for $\Delta V(K)$ and equals -5.5 ± 1.0 cm^3 mol^{-1}. Thus ion-pair formation between cytochrome c^{II} and $[Co(ox)_3]^{3-}$ must involve a significant overlap of the van der Waals radii of the reactants without significant charge neutralization which would induce desolvation. The ion-pair can then be depicted as solvent separated. The $\Delta V^{\#}(k_{ET})$ value of -5.5 ± 1.0 cm^3 mol^{-1} indicates that the transition state for the electron transfer reaction within the precursor (ion-pair) complex is more compact, which is most probably related to a volume decrease on the $[Co^{III}(ox)_3]^{3-}$ partner. As we showed earlier, the oxidation of cytochrome c^{II} to c^{III} is accompanied by a volume increase of 5 cm^3 mol^{-1} [52]. When $[Co^{III}(ox)_3]^{3-}$ is reduced to $[Co^{II}(ox)_3]^{4-}$, the increase in overall negative charge will cause an increase in electrostriction which could account for the observed negative volume of activation.

Recent investigations on a series of intramolecular electron transfer reactions, closely related to the series of intermolecular reactions described above, revealed non-symmetrical volume profiles [58]. Reactions of the type shown in Reaction 15

$$(NH_3)_4(L)Ru^{III}-(His33)-\text{cyt } c^{II} \rightleftharpoons (NH_3)_4(L)Ru^{II}-(His33)-\text{cyt } c^{III} \quad (15)$$

where L = isonicotinamide, 4-ethylpyridine, 3,5-lutidine, and pyridine, all exhibited volumes of activation for the forward reaction of between +3 and +7 cm^3 mol^{-1}, compared to overall reaction volumes of between +19 and +26 cm^3 mol^{-1}. This indicates that electron transfer from Fe to Ru is characterized by an 'early' transition state in terms of volume changes

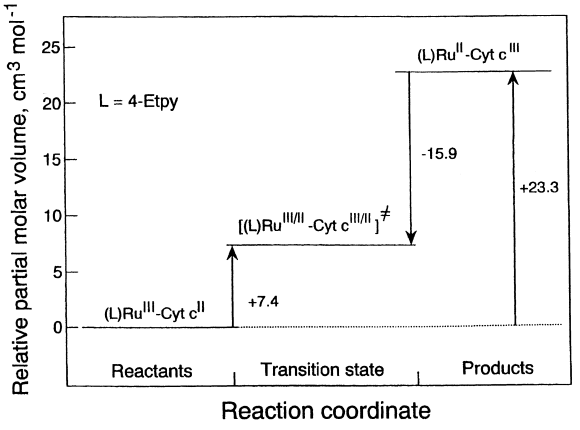

Fig. 8. Volume profile for the reaction $(NH_3)_4Ru^{III}$(4-Etpy)-cyt $c^{II} \rightleftharpoons (NH_3)_4Ru^{II}$(4-Etpy)-cyt c^{III}.

along the reaction coordinate (see Fig. 8). The overall volume changes could be accounted for in terms of electrostriction effects centered around the ammine ligands on the ruthenium center. A number of possible explanations in terms of the effect of pressure on electronic and nuclear factors were offered to account for the asymmetrical nature of the volume profile [58].

One system has been investigated where the effect of pressure on the electron-transfer rate constant revealed information on the actual electron-transfer route. In this study the effect of pressure on distant electronic coupling in Ru(bpy)$_2$(im)-modified His33 and His72 cytochrome *c* derivatives, for which the electron transfer from Fe(II) to Ru(III) is activationless [59]. In the case of the His33-modified system the electron-transfer rate constant exhibited no dependence on pressure within experimental error limits. However, the rate constant for the His72-modified protein increased significantly with increasing pressure, corresponding to a $\Delta V^{\#}$ value of -6 ± 2 cm^3 mol^{-1}. Since this value is exactly opposite to that expected for the reduction of Ru(III), the result was interpreted as an increase in electronic coupling at elevated pressure. The application of moderate pressures will cause a slight compression of the protein that in turn shrinks the through-space gaps that are key units in the electron-tunneling pathway between the heme and His72. A decrease of 0.46 A in the tunneling path length at a pressure of 150 MPa can account for the observed increase in rate constant. This in turn means that there is an average

Table 1
Activation and reaction volumes for typical outer-sphere electron transfer reactions

Reaction	$\Delta V^{\#}$, cm^3 mol^{-1}	ΔV, cm^3 mol^{-1}	Ref.
$[Co(NH_3)_5OH_2]^{3+}$+$[Fe(CN)_6]^4$	+26.5 ± 2.4	−15 ± 8	[38]
$[Co(NH_3)_5py]^{3+}$+$[Fe(CN)_6]^{4-}$	+29.8 ± 1.4	+23 ± 3	[38]
$[Co(NH_3)_5Me_2SO]^{3+}$+$[Fe(CN)_6]^{4-}$	+6 ± 2	−11 ± 3	[38]
$[Co(NH_3)_5(HP_2O_7)]$+$[Fe(CN)_6]^{4-}$	+36 ± 3 (308 K)	–	[41]
$[Co(NH_3)_5(P_2O_7)]^-$+$[Fe(CN)_6]^{4-}$	+13 ± 1 (314 K)	–	[41]
β-$[Co(NH_3)_5(P_3O_{10})]^{2-}$+$[Fe(CN)_6]^{4-}$	+13 ± 2 (308 K)	–	[41]
γ-$[Co(NH_3)_5(P_3O_{10})]^{2-}$+$[Fe(CN)_6]^{4-}$	+32 ± 2 (317 K)	–	[41]
$[Co(NH_3)_5(HPO_3)]^+$+$[Fe(CN)_6]^{4-}$	+22 ± 2 (314 K)	–	[41]
$[Co(NH_3)_5(H_2PO_2)]^{2+}$+$[Fe(CN)_6]^{4-}$	+30 ± 1 (314 K)	–	[41]
$[Co(NH_3)_5(HPO_4)]^+$+$[Fe(CN)_6]^{4-}$	+37 ± 4	–	[42]
$[Co(NH_3)_5(PO_4)]$+$[Fe(CN)_6]^{4-}$	+17 ± 1	–	[42]
$[Co(NMeH_2)_5(HPO_4)]^+$+$[Fe(CN)_6]^{4-}$	+44 ± 5	–	[42]
$[Co(NMeH_2)_5(PO_4)]$+$[Fe(CN)_6]^{4-}$	+32 ± 1	–	[42]
$[CoL(HPO_4)]^{+}$[a]+$[Fe(CN)_6]^{4-}$	+36 ± 2	–	[42]
L-Ascorbic acid+$[Fe(CN)_6]^{3-}$	−16.6 ± 0.5 (pH 0.3)	–	[44]
	−15 ± 1 (pH 5)	–	[44]
	−16.3 ± 0.4 (pH 5.25)	–	[44]
L-Ascorbic acid+$[Fe(CN)_5(NO_2)]^{3-}$	−10.0 ± 0.5	–	[45]
$[Ru(NH_3)_6]^{2+}$+cyt c^{III}	−15.6 ± 0.6	–	[49]
$[Ru(NH_3)_5isn]^{3+}$+cyt c^{II}	+15.9 ± 0.7	–	[50]
$[Ru(NH_3)_5isn]^{2+}$+cyt c^{III}	−17.2 ± 1.5	–	[50]
$[Ru(NH_3)_5lut]^{3+}$+cyt c^{II}	+16.9 ± 1.4	33.6 ± 1.7	[51]
$[Ru(NH_3)_5lut]^{2+}$+cyt c^{III}	−17.8 ± 1.6	34.7 ± 2.1	[51]
$[Ru(NH_3)_5etpy]^{3+}$+cyt c^{II}	+14.7 ± 1.8	26.9 ± 1.8	[51]
$[Ru(NH_3)_5etpy]^{2+}$+cyt c^{III}	−14.9 ± 1.1	29.6 ± 1.4	[51]
$[Ru(NH_3)_5py]^{3+}$+cyt c^{II}	+17.4 ± 1.5	33.4 ± 1.9	[51]
$[Ru(NH_3)_5py]^{2+}$+cyt c^{III}	−17.7 ± 0.8	35.1 ± 1.7	[51]
$[Co(bpy)_3]^{3+}$+cyt c^{II}	+12.5 ± 0.9	21.8 ± 0.7	[54]
$[Co(bpy)_3]^{2+}$+cyt c^{III}	−12.6 ± 1.5	25.1 ± 1.7	[54]
$[Co(phen)_3]^{3+}$+cyt c^{II}	+17.0 ± 0.9	37.9 ± 2.0	[54]
$[Co(phen)_3]^{2+}$+cyt c^{III}	−16.2 ± 1.0	34.2 ± 1.7	[54]
$[Co(terpy)_3]^{3+}$+cyt c^{II}	+18.4 ± 1.2	33 ± 3	[54]
$[Co(terpy)_3]^{2+}$+cyt c^{III}	−18.0 ± 1.4	36 ± 2	[54]
$[Cr^V]^-$+cyt c^{II}	−11.1 ± 0.8 (pH 4.7)	−9.7 ± 2.5 (pH 4.7)	[56]
	−9.2 ± 0.6 (pH 5)	−6.8 ± 2.3 (pH 5)	[56]
$[Co(ox)_3]^{3-}$+cyt c^{II}	−5.5 ± 1.0 (for k_{et})	−5.4 ± 1.6 (for K)	[57]
HAO+cyt c^{III}	−27.7 (I = 20 mM, T = 4°C)	–	[62]
	−24.3 (I = 20 mM, T = 20°C)	–	[62]
	−5.6 (I = 420 mM, T = 20°C)	–	[62]
MDH+cyt $c_L{}^{III}$	+122 (I = 20 mM, T = 4°C)	–	[62]
	+54 (I = 10 mM, T = 25°C)	–	[62]
	+70 (I = 110 mM, T = 25°C)	–	[62]

[a] L = *cis*-10-Amino-10-methyl-1,4,8,12-tetraazacyclopentadecane.

decrease in the space-gap of 0.1 A. The absence of an effect for the His33-modified species is understandable since electronic coupling through covalent and hydrogen bonds will be less pressure sensitive than coupling via van der Waals gaps [59].

Morishima and co-workers [60] investigated the effect of pressure on electron transfer rates in zinc/ruthenium modified myoglobins. The rate constant for electron transfer from photoexcited ^{3}ZnP* to a covalently attached $[Ru(NH_3)_5]^{3+}$ moiety on the surface of the protein decreased from 5×10^7 to 55 s^{-1} upon increasing the distance from 9.5 to 19.3 Å when

the Ru complex is attached to His70 and His83, respectively. This decrease in the rate constant was accompanied by an increase in $\Delta V^{\#}$ from +4 to +17 cm^3 mol^{-1}. Within the context of the results reported above and the volume changes associated with the reduction of the Ru(III) ammine complexes, the gradual increase in $\Delta V^{\#}$ with increasing donor-acceptor distance and with decreasing rate constant could be a clear demonstration of 'early' (for the fast) and 'late' (for the slow reactions) transition states. Volume changes mainly associated with changes in electrostriction on the Ru ammine center will control the solvent reorganization and so account for the 'early' (reactant-like) and 'late' (product-like) transition states.

Recently, Morishima and co-workers [61] re-examined their earlier results for electron transfer reactions within myoglobin derivatives [60]. They found that the differences in the activation volumes determined before, are wrong due to significant contributions from dissolved oxygen. The dissolved oxygen in the sample enhanced the decay of the triplet exited state of ZnMb. The results under completely anaerobic conditions show a negative activation volume for the forward reaction in the case of His83-Mb. The pathways of electron transfer in His83-Mb and His81-Mb are very similar constructed by many hydrogen bonds. Both histidines are exposed to the solvent, however hydrogen bonds of His81-Mb restrain the thermal fluctuations near His81, which is reflected in the reduced pressure perturbation on the D-A distance of His81-Mb. The pressure dependence of the electron transfer reaction is sensitive to slight structural deviations of the redox center. The D-A distance is shorter for His48-Mb, for which $\Delta V_f^{\#}$ was found to be positive. The $\Delta V_b^{\#}$ values for the backward reactions in all three derivatives were found to be negative.

Balny and co-workers have studied the effect of pressure on many protein-protein electron transfer processes, for which they also studied the effect of temperature and ionic strength. For the reduction of cytochrome *c* by hydroxylamine oxidoreductase, the activation volume is independent of temperature, but strongly dependent on the ionic strength. With decreasing ionic strength, the activation volume becomes more negative. At higher ionic strength, solvational effects play a more important role and the activation volume is more positive. Another behavior was observed for the reaction of methanol dehydrogenase with cytochrome c_L (both isolated from the *Methylophaga marina*). Values of the activation vol-

Table 2
Activation and reaction volumes for typical inner-sphere electron transfer reactions

Reaction	$\Delta V^{\#}$, cm^3 mol^{-1}	ΔV, cm^3 mol^{-1}	Ref.
(hh)[a]cyt c^{III}–$(NH_3)_5Ru^{II}$–His33	−17.7 ± 0.9	–	[49]
(Ck)[b]cyt c^{III}–$(NH_3)_5Ru^{II}$–His39	−18.3 ± 0.7	–	[49]
(hh)[a]cyt c^{III}–$(NH_3)_4$(isn)Ru^{II}	+3.2 ± 0.3	+21.1 ± 1.0	[58]
(hh)[a]cyt c^{III}–$(NH_3)_4$(Etpy)Ru^{II}	+7.4 ± 0.6	+24.9 ± 1.1	[58]
(hh)[a]cyt c^{III}–$(NH_3)_4$(lut)Ru^{II}	+5.8 ± 0.4	+23.3 ± 0.9	[58]
(hh)[a]cyt c^{III}–$(NH_3)_4$(py)Ru^{II}	+7.2 ± 0.2	+23.3 ± 0.6	[58]
MbZnP–$(NH_3)_5Ru^{III}$(His48)	+6	–	[60]
MbZnP–$(NH_3)_5Ru^{III}$(His70)	+4	–	[60]
MbZnP–$(NH_3)_5Ru^{III}$(His81)	+17	–	[60]
MbZnP–$(NH_3)_5Ru^{III}$(His83)	+9	–	[60]
MbZnP–$(NH_3)_5Ru^{III}$(His48)	+6.5 ± 1.0	–	[61]
MbZnP–$(NH_3)_5Ru^{II}$(His48)	−6.2 ± 0.5	–	[61]
MbZnP–$(NH_3)_5Ru^{III}$(His81)	+3.7 ± 0.1	–	[61]
MbZnP–$(NH_3)_5Ru^{II}$(His81)	−5.3 ± 0.5	–	[61]
MbZnP–$(NH_3)_5Ru^{III}$(His83)	−1.6 ± 0.2	–	[61]
MbZnP–$(NH_3)_5Ru^{II}$(His83)	−11.0 ± 0.5	–	[61]
cyt a_3–cyt *a*	+41 ± 5		[63]
cyt *a*–Cu_A	+28 ± 4		[63]

[a](hh), horse heart.
[b](Ck), *Candida krusei*.

ume depend on the temperature. In the Arrhenius plot a break is observed, which was interpreted as resulting from the existence of two different conformations of cytochrome c_L [62].

Larsen [63] used a pressure-dependent transient absorption spectroscopy technique for studying the intramolecular electron transfer reaction in CO-mixed derivative of bovine heart cytochrome *c* oxidase (CcO). Two phases of electron transfer were distinguished. The first one is the fast intramolecular ET between cytochrome *a* and cytochrome a_3. The rate constant $k_{et} = (6.7 \pm 0.9) \times 10^5$ s^{-1} and activation volume $\Delta V^{\#} = +45 \pm 5$ cm^3 mol^{-1} were determined. The value of $\Delta V^{\#}$ for this process arises from the structural changes localized at cytochrome a_3 upon heme reduction. The second phase is a slow electron transfer process between cytochrome *a* and Cu_A. The rate constant k_{et} was found to be $(5.9 \pm 1.7) \times 10^4$ s^{-1} at ambient pressure while $\Delta V^{\#} = +28 \pm 4$ cm^3 mol^{-1}. The activation volume results from structural changes at Cu_A during the reduction. The conformation regulation during electron transfer reaction was not observed on the surface of cytochrome *a*. Information about conformational changes upon reduction resulted from the crystal structures of reduced and oxidized forms of these cytochromes. Analysis of similar examples from the literature suggested that in the presented system the activation volume for the intramolecular electron transfer process depends on two contributions, viz. reorganization ($\Delta V^{\#}_{FC}$) and electronic coupling ($\Delta V^{\#}_{EC}$) terms.

6. Conclusions

Studies on the effect of pressure on electron transfer reactions can assist the elucidation of the intimate reaction mechanism of such processes. The experimental data for symmetrical (self exchange) electron transfer reactions only allow the interpretation of activation volumes, which turn out to be in good agreement with theoretical predictions. In the case of non-symmetrical electron transfer reactions, the first objective is to distinguish between intramolecular and intermolecular processes. A summary of the available activation and reaction volumes for typical outer-sphere and inner-sphere electron transfer reactions is given in Tables 1 and 2, respectively. When the electron transfer reaction is reversible, it is in some cases possible to study the reaction in both the forward and backward directions and to construct a volume profile. For reactions that occur irreversibly, it is more difficult to determine all the parameters that are necessary to construct a volume profile. Nevertheless, these problems can be overcome in some cases by using alternative techniques such as electrochemical measurements at elevated pressure. The application of high pressure does not only contribute to an improved mechanistic understanding of electron transfer reactions in model inorganic systems, but can also contribute to the understanding of more complex processes as found in long distance electron transfer reactions in biological systems.

Acknowledgements

The authors gratefully acknowledge financial support from the Deutsche Forschungsgemeinschaft and the Volkswagen Foundation.

References

[1] D.R. Stranks, Pure Appl. Chem. 38 (1974) 303–323.
[2] H. Kelm, High Pressure Chemistry, Reidel, Dordrecht, 1978.
[3] R. van Eldik, Inorganic High Pressure Chemistry, Kinetics and Mechanism, Elsevier, Amsterdam, 1986.
[4] R. van Eldik, J. Jonas, High Pressure Chemistry and Biochemistry, Reidel, Dordrecht, 1987.
[5] M. Kotowski, R. van Eldik, Coord. Chem. Rev. 93 (1989) 19–57.
[6] R. van Eldik, T. Asano, W.J. le Noble, Chem. Rev. 89 (1989) 549–688.
[7] J.W. Akitt, A.E. Merbach, NMR Basic Princ. Prog. 24 (1990) 189.
[8] R. van Eldik, A.E. Merbach, Comments Inorg. Chem. 12 (1992) 341.
[9] S.F. Lincoln, A.E. Merbach, Adv. Inorg. Chem. 42 (1995) 1.
[10] L. Helm, A.E. Merbach, Coord. Chem. Rev. 187 (1999) 151–181.
[11] G. Stochel, R. van Eldik, Coord. Chem. Rev. 187 (1999) 329–374.
[12] T.W. Swaddle, P.A. Tregloan, Coord. Chem. Rev. 187 (1999) 255–289.
[13] R. Winter, J. Jonas, High Pressure Chemistry, Biochemistry and Materials Science, Kluwer, Dordrecht, 1993.
[14] C.D. Hubbard, R. van Eldik, Instrum. Sci. Technol. 23 (1995) 1–41.

[15] R. van Eldik, C.D. Hubbard, Chemistry under Extreme or Non-Classical Conditions, Wiley/Spektrum, New York/Heidelberg, 1997.
[16] W.R. Holzapfel, N.S. Isaacs, High Pressure Techniques in Chemistry and Physics, Oxford University Press, Oxford, 1997.
[17] R. van Eldik, in: D. Nocera, J.F. Wishart (Eds.), Photochemistry and Radiation Chemistry: Complementary Methods in the Study of Electron Transfer, Adv. Chem. Series 254, Washington, DC, 1998.
[18] W.H. Jolley, D.R. Stranks, T.W. Swaddle, Inorg. Chem. 29 (1990) 1948–1951.
[19] H. Takagi, T.W. Swaddle, Inorg. Chem. 31 (1992) 4669–4673.
[20] L. Spiccia, T.W. Swaddle, Inorg. Chem. 26 (1987) 2265–2271.
[21] H. Doine, T.W. Swaddle, Inorg. Chem. 30 (1991) 1858–1862.
[22] R.D. Shalders, T.W. Swaddle, Inorg. Chem. 34 (1995) 4815–4820.
[23] W.H. Jolley, D.R. Stranks, T.W. Swaddle, Inorg. Chem. 29 (1990) 385–389.
[24] M.R. Grace, T.W. Swaddle, Inorg. Chem. 32 (1993) 5597–5602.
[25] T.W. Swaddle, Inorg. Chem. 29 (1990) 5017–5025.
[26] M.R. Grace, H. Takagi, T.W. Swaddle, Inorg. Chem. 33 (1994) 1915–1920.
[27] T.W. Swaddle, High Pressure Inorganic Chemistry: Kinetics and Mechanisms, Elsevier, Amsterdam, 1987.
[28] B. Goyal, S. Solanki, S. Arora, A. Prakash, R.N. Mehotra, J. Chem. Soc. Dalton Trans. (1995) 3109.
[29] J.M. Leal, P.L. Domingo, B. Garcia, S. Ibeas, J. Chem. Soc. Faraday Trans. 89 (1995) 3571.
[30] P.D. Metelski, T.W. Swaddle, Inorg. Chem. 38 (1999) 301–307.
[31] C.D. Hubbard, A. Gerhard, R. van Eldik, unpublished observation.
[32] Y. Fu, T.W. Swaddle, Chem. Commun. (1996) 1171-1172.
[33] T.W. Swaddle, Can. J. Chem. 74 (1996) 631–638.
[34] Y. Fu, T.W. Swaddle, J. Am. Chem. Soc. 119 (1997) 7137–7144.
[35] J.I. Sachinidis, R.D. Shalders, P.A. Tregloan, Inorg. Chem. 33 (1994) 6180–6186.
[36] J.I. Sachinidis, R.D. Shalders, P.A. Tregloan, Inorg. Chem. 35 (1996) 2497–2503.
[37] R. van Eldik, High Press. Res. 6 (1991) 251.
[38] I. Krack, R. van Eldik, Inorg. Chem. 25 (1986) 1743–1747.
[39] I. Krack, R. van Eldik, Inorg. Chem. 29 (1989) 851–855.
[40] I. Krack, R. van Eldik, Inorg. Chem. 29 (1990) 1700–1704.
[41] M. Martinez, M.-A. Pitarque, R. van Eldik, J. Chem. Soc. Dalton Trans. (1996) 2665-2671.
[42] M. Martinez, M.-A. Pitarque, R. van Eldik, J. Chem. Soc. Dalton Trans. (1995) 4107.
[43] M. Martinez, M.-A. Pitarque, R. van Eldik, Inorg. Chim. Acta 256 (1997) 51–59.
[44] B. Bänsch, P. Martinez, J. Zuluaga, D. Uribe, R. van Eldik, Z. Phys. Chem. 170 (1991) 59–71.
[45] A. Wanat, R. van Eldik, G. Stochel, J. Chem. Soc. Dalton Trans. (1998) 2497-2501.
[46] M. Matsumoto, T. Tarumi, K.-I. Sugimoto, N. Kagayama, S. Funahashi, H.D. Takagi, Inorg. Chim. Acta 255 (1997) 81.
[47] E. Ilkowska, R. van Eldik, G. Stochel, J. Biol. Inorg. Chem. 2 (1992) 603.
[48] H.-D. Projahn, C. Dreher, R. van Eldik, J. Am. Chem. Soc. 112 (1990) 17–22.
[49] J.F. Wishart, R. van Eldik, J. Sun, C. Su, S.S. Isied, Inorg. Chem. 31 (1992) 3986–3989.
[50] B. Bänsch, M. Meier, P. Martinez, R. van Eldik, C. Su, J. Sun, S.S. Isied, J.F. Wishart, Inorg. Chem. 33 (1994) 4744–4749.
[51] M. Meier, J. Sun, R. van Eldik, J.F. Wishart, Inorg. Chem. 35 (1996) 1564–1570.
[52] J. Sun, J.F. Wishart, R. van Eldik, R.D. Shalders, T.W. Swaddle, J. Am. Chem. Soc. 117 (1995) 2600–2605.
[53] M. Meier, R. van Eldik, Inorg. Chim. Acta 225 (1994) 95.
[54] M. Meier, R. van Eldik, Chem. Eur. J. 3 (1997) 39–46.
[55] M.T. Cruanes, K.K. Rodgers, S.G. Sligar, J. Am. Chem. Soc. 114 (1992) 9660–9661.
[56] M. Körner, R. van Eldik, Eur. J. Inorg. Chem. (1999) 1805-1812.
[57] J. Macyk, R. van Eldik, J. Chem. Soc. Dalton Trans. (2001) 2288-2292.
[58] J. Sun, C. Su, M. Meier, S.S. Isied, J.F. Wishart, R. van Eldik, Inorg. Chem. 37 (1998) 6129–6135.
[59] M. Meier, R. van Eldik, I.J. Chang, G.A. Mines, D.S. Wuttke, J.R. Winkler, H.B. Gray, J. Am. Chem. Soc. 116 (1994) 1577–1578.
[60] Y. Sugiyama, S. Takahashi, K. Ishimori, I. Morishima, J. Am. Chem. Soc. 119 (1997) 9582–9583.
[61] Y. Furukawa, K. Ishimori, I. Morishima, J. Phys. Chem. 104 (2000) 1817.
[62] C. Balny, High Pressure and Biotechnology., Vol. 224, Editions John Libbey Eurotext, Montrouge, 1992, pp. 155–157.
[63] R.W. Larsen, FEBS Lett. 462 (1999) 75–78.